Research Article

Quality and Reliability Engineering International

(wileyonlinelibrary.com) DOI: 10.1002/qre.1397

Published online 17 April 2012 in Wiley Online Library

Yield-Related Process Capability Indices for Processes of Multiple Quality Characteristics

Jyh-Jen Horng Shiau,[a]*† Chia-Ling Yen,[a] W. L. Pearn[b] and Wan-Tsz Lee[a]

Process capability indices (PCIs) have been widely used in industries for assessing the capability of manufacturing processes. Castagliola and Castellanos (*Quality Technology and Quantitative Management* 2005, 2(2):201–220), viewing that there were no clear links between the definition of the existing multivariate PCIs and theoretical proportion of nonconforming product items, defined a bivariate C_{pk} and C_p (denoted by BC_{pk} and BC_p, respectively) based on the proportions of nonconforming product items over four convex polygons for bivariate normal processes with a rectangular specification region. In this paper, we extend their definitions to MC_{pk} and MC_p for multivariate normal processes with flexible specification regions. To link the index to the yield, we establish a 'reachable' lower bound for the process yield as a function of MC_{pk}. An algorithm suitable for such processes is developed to compute the natural estimate of MC_{pk} from process data. Furthermore, we construct via the bootstrap approach the lower confidence bound of MC_{pk}, a measure often used by producers for quality assurance to consumers. As for BC_p, we first modify the original definition with a simple preprocessing step to make BC_p scale-invariant. A very efficient algorithm is developed for computing a natural estimator $\hat{BC}_p$ of BC_p. This new approach of BC_p can be easily extended to MC_p for multivariate processes. For BC_p, we further derive an approximate normal distribution for $\hat{BC}_p$, which enables us to construct procedures for making statistical inferences about process capability based on data, including the hypothesis testing, confidence interval, and lower confidence bound. Finally, the proposed procedures are demonstrated with three real data sets. Copyright © 2012 John Wiley & Sons, Ltd.

Keywords: multivariate process capability indices; yield assurance index; normal approximation; lower confidence bound; bootstrap

1. Introduction

Process capability indices (PCIs) are some measures developed for engineering convenience to quantify process performances. Facing stronger-than-ever competitions nowadays, manufacturing companies must assure product quality to their customers to stay competitive. By revealing how well the actual process is in conformance with the manufacturing specifications, PCIs have been widely used in industries as a metric of quality assurance in recent years, and the role is becoming more and more important.

Univariate PCIs have been extensively studied in the literature. Some indices such as C_p, C_{pu}, C_{pl}, C_{pk}, C_{pm}, and C_{pmk} have shown good values in evaluating univariate processes. See, for example, Kane,[1] Chan *et al.*,[2] Pearn *et al.*,[3] Kotz and Johnson,[4] Kotz and Lovelace,[5] and Pearn and Kotz.[6]

In many applications, especially in high-technology industries, processes are so complex that the product quality often is affected by multiple characteristics simultaneously. As a result, appropriate multivariate PCIs for assessing processes/products of more than one quality characteristic are desirable. Nonetheless, multivariate PCIs have received comparatively a lot less attention than univariate PCIs in the literature.

In recent years, more and more studies have been devoted to multivariate PCIs. Chan *et al.*[7] extended their univariate index C_{pm} in Chan *et al.*[2] to a multivariate version by measuring how far away from the target vector the process mean is in the Mahalanobis distance. Pearn *et al.*[3] proposed a multivariate version of C_p and C_{pm} with an approach they claimed to be more natural than that of Chan *et al.*[7] Hubele *et al.*[8] proposed a process capability vector for bivariate normal processes, and later, Shahriari *et al.*[9] extended it to the multivariate case. Taam *et al.*[10] proposed a multivariate C_p as the ratio of two areas, the area of a modified specification (also called the modified engineering tolerance region by some researchers), defined as the largest ellipsoid centering at the target value and completely within the original specification over the area of the elliptical process region that covers 99.73% of the multivariate normal process. Considering the possible shift of the process mean from the target vector, Taam *et al.*[10] further modified this index by taking into account an adjustment factor that measures the closeness between the process mean and the target vector to define a

[a]*Institute of Statistics, National Chiao Tung University, Hsinchu, Taiwan*
[b]*Department of Industrial Engineering and Management, National Chiao Tung University, Hsinchu, Taiwan*
**Correspondence to: Jyh-Jen Horng Shiau, Institute of Statistics, National Chiao Tung University, Hsinchu, Taiwan.*
†*E-mail: jyhjen@stat.nctu.edu.tw*

multivariate C_{pm} index exactly the same way as Pearn *et al*.[3] Recently, Pan and Lee[11] revised Taam *et al*.'s modified engineering tolerance region by taking into account the correlation between multiple quality characteristics and proposed two new multivariate PCIs for C_p and C_{pm}, respectively, which could reflect more correctly the process precision and accuracy. Chen[12] proposed a multivariate PCI using the concept of a tolerance zone, which allows flexible specifications and no assumptions on the process distribution. Pal[13] proposed a bivariate PCI as the ratio of the area of the specification rectangle and the 99.73% area of the process region, similar to the index proposed by Taam *et al*.[10] Bothe[14] proposed a multivariate C_{pk} index defined as $Z_P/3$, where P is the conforming proportion and Z_P is the Pth quantile of the standard normal distribution. Wang *et al*.[15] compared three multiple PCIs proposed by Taam *et al*.,[10] Chen,[12] and Shahriari *et al*.,[9] respectively, via graphical and computational examples. Wang and Chen[16] and Wang and Du[17] proposed multivariate PCIs using principal component analysis (PCA). Recently, Shinde and Khadse[18] pointed out that the specification region corresponding to the principal components used in Wang and Chen's PCI definition was not correct and suggested an alternative method for assessing multivariate process capability based on the empirical probability distribution of principal components. In an earlier work, Shinde and Khadse[19] reviewed and compared some multivariate PCIs based on fraction conforming interpretation. Gonzalez and Sanchez,[20] by relating the actual variability of the process with the prespecified nonconforming proportion, proposed a unitary PCI that can be applied to non-centered univariate processes as well as to general multivariate processes.

Among univariate PCIs, C_{pk} could be the most popular one, not only because it accounts for both process mean and variance when assessing the process capability but probably also because it links directly to the process yield by the following inequality given in Boyles:[21]

$$2\Phi\left(3C_{pk}\right) - 1 \leqslant \%\text{yield} \leqslant \Phi\left(3C_{pk}\right), \tag{1}$$

where %yield stands for the process yield, and $\Phi(\cdot)$ is the cumulative distribution function (c.d.f.) of the standard normal distribution. Therefore, C_{pk} is sometimes referred to as a yield assurance index. It is well known that the lower bound, $2\Phi(3C_{pk}) - 1$, is not a trivial bound; instead, it is a 'reachable' lower bound in the sense that it can be reached by some processes.

However, in the literature, the link between multivariate PCIs and the product yield was seldom emphasized. One exception was the work of Castagliola and Castellanos.[22] Castagliola and Castellanos,[22] viewing that there were no clear links between the definition of the existing multivariate PCIs and theoretical proportion of nonconforming product items, defined two indices, BC_{pk} and BC_p, based on the proportions of nonconforming product items over four convex polygons for bivariate normal processes with a rectangular specification region. This definition of BC_{pk} is rather interesting because it accounts for the relative position and the orientation of the process distribution with respect to the specification region. Specifically, as an extension of C_{pk}, BC_{pk} quantifies the process capability based on the smallest conforming proportion of the four convex polygons formed by dividing the rectangular specification region with the two main axes (i.e., the principal components) of the process distribution.

As defined by Castagliola and Castellanos,[22] the relationship between BC_{pk} and BC_p is analogous to that between the univariate C_{pk} and C_p. Specifically, because the notion of C_p only concerns with the process variability, BC_p was defined as the maximum BC_{pk} value of all bivariate normal distributions with the same covariance matrix as the process covariance matrix Σ, which is analogous to the univariate case. Although this definition works for the univariate case, unfortunately it fails the scale-invariance property for multivariate processes. As a result, the value of BC_p is not consistent when quality characteristics are measured in different units or scales.

The main purpose of this paper is to extend the notion of BC_{pk} and BC_p to multivariate PCIs (denoted by MC_{pk} and MC_p, respectively) for multivariate processes that may have more than two quality characteristics. We first define MC_{pk} and then establish the same 'reachable' lower bound for the process yield in terms of MC_{pk} as in (1). Because the computation method of Castagliola and Castellanos[22] is only for bivariate processes with rectangular specification regions, we further develop a computation method that can be implemented for multivariate processes with flexible specification regions. As for BC_p, we modify the definition of Castagliola and Castellanos[22] with a simple preprocessing step; then BC_p becomes scale-invariant. Also, because the computation method provided in Castagliola and Castellanos[22] for $\hat{BC}_p$, a natural estimate of BC_p, is very time-consuming, a very efficient algorithm is developed. Moreover, we derive an approximate distribution for $\hat{BC}_p$, which enables us to provide statistical procedures for making inferences about process capability based on data, including hypothesis testing, confidence interval (CI), and lower confidence bound. The results of statistical inferences are very useful in decision making. In particular, the lower confidence bound is a measure of high practical value because it directly links to the quality assurance. Finally, we also extend BC_p to MC_p for multivariate processes.

The rest of the paper is organized as follows. In Section 2, we first review the index BC_{pk} proposed by Castagliola and Castellanos[22] for bivariate processes. Then, we establish the link between this index and the product yield. We further extend this index to multivariate processes of more than two characteristics. After that, we give an algorithm for the estimation of MC_{pk} and propose obtaining lower confidence bounds by bootstrap methods. For demonstration, we apply the methods to simulated examples in the bivariate case. We also study the distribution of a natural estimator of BC_{pk} by simulation. In Section 3, for BC_p, we show how to obtain a scale-invariant BC_p and how and why $\hat{BC}_p$ can be efficiently calculated. We further derive an approximate normal distribution for $\hat{BC}_p$ and then use it to construct statistical procedures for inferences about process capability. In Section 4, as illustrative examples, we apply the proposed indices and inference procedures to the two sets of real (bivariate) data presented in Castagliola and Castellanos[22] and a trivariate dataset obtained from a stencil printing process described in Pan and Lee.[11] Finally, we conclude the paper with a brief summary and remark in Section 5.

2. Multivariate C_{pk} index–a yield measuring process capability index

2.1. Alternative definition for C_{pk}

Assume that the quality characteristic X of a product item follows a normal distribution with mean μ and variance σ^2, denoted by $N(\mu, \sigma^2)$. Let $[LSL, USL]$ be the corresponding lower and upper specification limits. The usual definition of C_{pk} as defined by Kane[1] is

$$C_{pk} = min\left\{\frac{USL-\mu}{3\sigma}, \frac{\mu-LSL}{3\sigma}\right\}, \tag{2}$$

which accounts for not only the spread of the process but also the location of the process mean relative to the specification limits. Equivalent to (2), an alternative definition for C_{pk} was proposed by Castagliola and Castellanos.[22] This definition is based on the lower and upper proportions of nonconforming product items, $p_L = P(X \leqslant LSL)$ and $p_U = P(X \geqslant USL)$, as follows. Because X follows $N(\mu, \sigma^2)$, $p_L = \Phi\left(-\frac{\mu-LSL}{\sigma}\right)$ and $p_U = \Phi\left(-\frac{USL-\mu}{\sigma}\right)$. Thus, C_{pk} is equivalent to

$$\frac{1}{3} min\left\{-\Phi^{-1}(p_L), -\Phi^{-1}(p_U)\right\}, \tag{3}$$

because of the fact that the c.d.f. $\Phi(\cdot)$ is a strictly increasing function. Similarly, the usual definition of $C_p = (USL - LSL)/6\sigma$ proposed by Kane[1] is equivalent to

$$\frac{1}{6}\left(-\Phi^{-1}(p_U) - \Phi^{-1}(p_L)\right).$$

2.2. Castagliola and Castellanos' definition of BC_{pk}

Let X_1 and X_2 be the quality characteristics of interest with the specification limits $[LSL_1, USL_1]$ for X_1 and $[LSL_2, USL_2]$ for X_2. These limits define a rectangular specification area. Assume that $X = (X_1, X_2)^T$ follows a bivariate normal distribution with mean $\mu = (\mu_1, \mu_2)^T$ and variance-covariance matrix Σ. Applying eigenvalue–eigenvector decomposition to Σ, one can obtain two eigenvalues, $\lambda_1^2 \geqslant \lambda_2^2 > 0$, and the associated eigenvectors, v_1 and v_2. Let $R = [v_1, v_2]$. Then $R^T R = I$ and Σ can be expressed as $\Sigma = RV R^T$, where V is the diagonal matrix with diagonal elements λ_1^2 and λ_2^2. In fact, the matrix R represents the rotation matrix that rotates the original axes to the main axes of the bivariate normal distribution (see Figure 1); the directions of the eigenvectors v_1 and v_2 correspond to the main axes; and λ_1^2 and λ_2^2 are the variances of X projected onto the two main axes, respectively. More specifically, if we let $S_i = v_i^T X$, then $S_i \sim N\left(v_i^T \mu, \lambda_i^2\right)$ for $i = 1, 2$; moreover, S_1 and S_2 are independent. In the PCA context, v_1 and v_2 are called principal components, and S_1 and S_2 are called principal component scores.

Suppose we move the origin to the process mean μ and rotate the two original axes to the directions of v_1 and v_2. Then, the two new axes divide the plane into four regions, A_1, A_2, A_3, and A_4. Obviously, $P(X \in A_i) = 1/4$ for $i = 1, 2, 3, 4$. Denote the specification region by A. Let $Q_i = A_i \cap A$ and $q_i = P(X \in Q_i)$ for $i = 1, 2, 3, 4$. Then, the probability that X is in A_i but not in the specification region A is $p_i = 1/4 - q_i$. See Figure 1. In other words, p_is are the proportions of nonconforming product items in the four quadrants of the new coordinate system.

By analogy to the alternative definition of C_{pk} given in (3), Castagliola and Castellanos[22] defined a bivariate C_{pk} as

$$BC_{pk} = \frac{1}{3} min\left\{-\Phi^{-1}(2p_1), -\Phi^{-1}(2p_2), -\Phi^{-1}(2p_3), -\Phi^{-1}(2p_4)\right\}. \tag{4}$$

This definition is similar to the univariate case as in (3), except that $0 \leqslant p_i \leqslant 1/4$ for $i = 1, 2, 3, 4$ in the bivariate case, whereas $0 \leqslant p_U$, $p_L \leqslant 1/2$ in the univariate case. We will extend this definition to higher dimensions later.

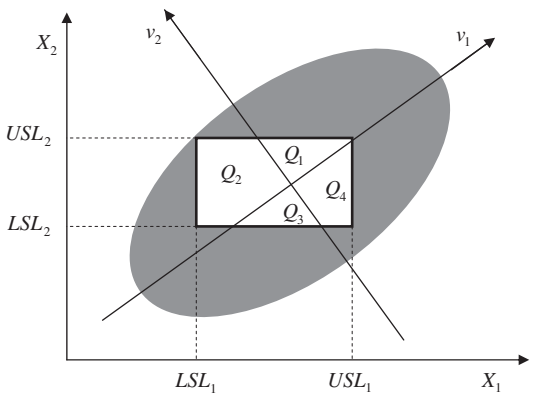

Figure 1. Explaining diagram of BC_{pk}

2.3. *Nonconforming rate based on BC_{pk}*

According to the definition of BC_{pk} in the last subsection, we can establish a link between the nonconforming rate (denoted by %*NC*) and BC_{pk} as follows. First note that, by (4),

$$BC_{pk} = -\frac{1}{3} max\left\{\Phi^{-1}(2p_1), \Phi^{-1}(2p_2), \Phi^{-1}(2p_3), \Phi^{-1}(2p_4)\right\}.$$

Because $\Phi^{-1}(\cdot)$ is a strictly increasing function, we have

$$BC_{pk} = -\frac{1}{3}\Phi^{-1}(2p_{max}), \tag{5}$$

where $p_{max} = max\{p_1, p_2, p_3, p_4\}$. Then, by (5),

$$p_{max} = \frac{1}{2}\Phi(-3BC_{pk}). \tag{6}$$

Note that $p_{max} \leqslant \%NC \leqslant 4p_{max}$. Plugging (6) into this inequality, we obtain

$$\frac{1}{2}\Phi(-3BC_{pk}) \leqslant \%NC \leqslant 2\Phi(-3BC_{pk}). \tag{7}$$

The upper bound in (7) is very useful and is not a loose bound, meaning that it is reachable for some processes. Usually, producers can take this upper bound as a metric of quality assurance to customers. For example, if the process is with $BC_{pk} = 1.00$, one can guarantee that there will be at most 2700 non-conformities in 1,000,000 product items. On the other hand, the lower bound in (7) is quite conservative; nevertheless, it is a convenient bound, meaning when a practitioner obtains a BC_{pk} value, a lower bound of the nonconforming rate as such is immediately available to him/her.

Table I gives the upper and lower bounds of the nonconforming rate %*NC* for various values of BC_{pk}. Figure 2 plots the bounds. We can see the bounds drop sharply as BC_{pk} increases and soon carried out to near zero level when $BC_{pk} \geq 1.5$.

The second inequality of (7) is equivalent to

$$2\Phi(3BC_{pk}) - 1 \leqslant \%\ \text{yield}, \tag{8}$$

which provides a 'reachable' lower bound for the yield. Note that this lower bound is the same as that in (1) for the univariate case. When the BC_{pk} value of the process is available, producers can assure the yield level with this lower bound to their customers.

2.4. *Extending BC_{pk}* to higher dimensions

We now generalize the alternative definition of BC_{pk} to multivariate processes of k characteristics where $k > 2$. By the same notion for the bivariate case, dividing the Euclidean space R^k into 2^k hyperquadrants by the k main axes (i.e., principal components) of the k-variate distribution, we can define a multivariate C_{pk} index as

$$\begin{aligned} MC_{pk} &= \frac{1}{3} min\left\{-\Phi^{-1}\left(2^{k-1}p_1\right), -\Phi^{-1}\left(2^{k-1}p_2\right), \ldots, -\Phi^{-1}\left(2^{k-1}p_{2^k}\right)\right\} \\ &= -\frac{1}{3} max\left\{\Phi^{-1}\left(2^{k-1}p_1\right), \Phi^{-1}\left(2^{k-1}p_2\right), \ldots, \Phi^{-1}\left(2^{k-1}p_{2^k}\right)\right\} \\ &= -\frac{1}{3}\Phi^{-1}\left(2^{k-1}p_{max}\right), \end{aligned} \tag{9}$$

where p_i is the probability of a randomly selected sample that is in the ith hyperquadrant but not in the specification region for $i = 1, 2, , 2^k$ and $p_{max} = max\left\{p_1, p_2, \ldots, p_{2^k}\right\}$. Equivalently,

Table I. Bounds of non-conformities based on BC_{pk}

	Non-conformities (in ppm)	
BC_{pk}	Lower bound	Upper bound
0.60	17965.15956	71860.63823
0.80	4098.76796	16395.07185
1.00	674.94902	2699.79606
1.33	16.51832	66.07330
1.50	1.69884	6.79535
1.60	0.39666	1.58666
1.67	0.13608	0.54430
2.00	0.00049	0.00197

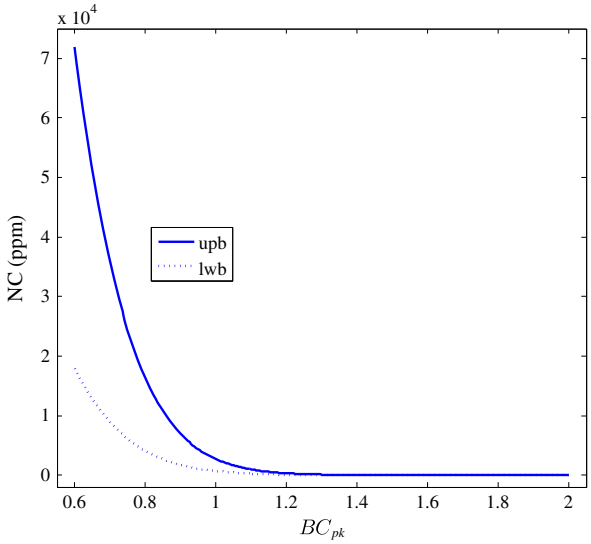

Figure 2. Bounds of non-conformities based on BC_{pk}

$$p_{\max} = \frac{1}{2^{k-1}}\Phi\left(-3MC_{\text{pk}}\right).$$

Because $p_{\max} \leqslant \%NC \leqslant 2^k p_{\max}$, we can also obtain bounds for the nonconforming rate in the general multivariate case as

$$\frac{1}{2^{k-1}}\Phi\left(-3MC_{\text{pk}}\right) \leqslant \%NC \leqslant 2\Phi\left(-3MC_{\text{pk}}\right), \tag{10}$$

which is equivalent to

$$2\Phi\left(3MC_{\text{pk}}\right) - 1 \leqslant \%\text{yield} \leqslant 1 - \frac{1}{2^{k-1}}\Phi\left(-3MC_{\text{pk}}\right). \tag{11}$$

2.5. *Estimation of MC_{pk}*

With the definition of MC_{pk} given in (9), a natural estimator of MC_{pk} is

$$\hat{MC}_{\text{pk}} = -\frac{1}{3}\Phi^{-1}\left(2^{k-1}\hat{p}_{\max}\right),$$

where $\hat{p}_{\max} = max\left\{\hat{p}_1, \hat{p}_2, \ldots, \hat{p}_{2^k}\right\}$ with $\hat{p}_i$ being the sample nonconforming proportion in the ith hyperquadrant for $i = 1, 2, \ldots, 2^k$.

The method to calculate $\hat{p}_i$ and $\hat{q}_i$ proposed by Castagliola and Castellanos[22] is a fairly complicated integration method that turns two-dimensional integrations over convex polygons into line integrals based on Green's formula, which cannot be directly extended to higher dimensions. Next, we propose an algorithm to calculate $\hat{MC}_{\text{pk}}$ from a sample of n k-dimensional quality characteristic vectors, $x_1, x_2, \ldots, x_n$.

Algorithm for Calculating $\hat{MC}_{\text{pk}}$:

1. Estimate μ and Σ by the usual sample mean and sample covariance matrix as

$$\hat{\mu} = \frac{1}{n}\sum_{j=1}^{n} x_j \quad \text{and} \quad \hat{\Sigma} = \frac{1}{n-1}\sum_{j=1}^{n}\left(x_j - \hat{\mu}\right)\left(x_j - \hat{\mu}\right)^T.$$

2. Compute eigenvalues $\hat{\lambda}_1^2, \hat{\lambda}_2^2, \ldots, \hat{\lambda}_k^2$ and eigenvectors $\hat{v}_1, \hat{v}_2, \ldots, \hat{v}_k$ of $\hat{\Sigma}$. (Denote by $A_1, A_2, \ldots, A_{2^k}$ the 2^k hyperquadrants of the Euclidean space R^k using the center $\hat{\mu}$ as the origin and the k orthogonal directions $\hat{v}_1, \hat{v}_2, \ldots, \hat{v}_k$ as the coordinate axes.)
3. Compute an estimate $\hat{p}_i$ of p_i for $i = 1, 2, \ldots, 2^k$ by Monte Carlo integration as follows. Generate $\{X_1, X_2, \ldots, X_N\}$, a very large number of data from $N_k\left(\hat{\mu}, \hat{\Sigma}\right)$. For each $X_j, j = 1, 2, \ldots, N$, determine which hyperquadrant it belongs to by the signs of $\left\{\left(X_j - \hat{\mu}\right)^T \hat{v}_l,\ l = 1, 2, \ldots, k\right\}$. Compute the proportion of X_js that are in the intersection of the specification region A and the ith hyperquadrant A_i by

$$\hat{q}_i = \frac{\sharp\{X_j \in A_i \cap A\}}{N} \tag{12}$$

and compute

$$\hat{p}_i = \frac{1}{2^k} - \hat{q}_i \quad \text{for} \quad i = 1, 2, \ldots, 2^k.$$

4. Compute $\hat{p}_{\max} = max\{\hat{p}_1, \hat{p}_2, \ldots, \hat{p}_{2^k}\}$ and then the estimate for MC_{pk} by

$$\hat{MC}_{\text{pk}} = -\frac{1}{3}\Phi^{-1}(2^{k-1}\hat{p}_{\max}).$$

We remark that despite requiring intensive computation for higher dimensions because of the curse of dimensionality, this Monte Carlo method works for all dimensions and any shapes of the specification region.

However, when studying the distribution of $\hat{MC}_{\text{pk}}$ empirically, we need to repeat the estimation procedure for each realization of $\hat{MC}_{\text{pk}}$. Then the algorithm described earlier becomes computationally infeasible because each replication would need the generation of a huge amount of data from its own $N_k(\hat{\mu}, \hat{\Sigma})$, say, $N = 1{,}000{,}000$ or even 10,000,000 in the bivariate case, for Monte Carlo integration; and a large number of replications are needed to obtain a good approximation. To overcome this computation difficulty, we develop a procedure that requires generating N data from the standard multivariate normal distribution $N_k(0, I)$ only once—which in turn can be carried out by simply generating $N \times k$ data from the (univariate) standard normal distribution—as described in the following.

Because Σ is assumed symmetric positive definite, there exists a unique symmetric positive definite matrix $\Sigma^{1/2}$ such that $\Sigma = (\Sigma^{1/2})(\Sigma^{1/2})$ (Golub and Van Loan,[23] p. 395). To simplify the notation, $(\Sigma^{1/2})^{-1}$ is denoted by $\Sigma^{-1/2}$. It is well known that the affine transformation of $Z = \Sigma^{-1/2}(X - \mu)$ transforms a random vector X following $N_k(\mu, \Sigma)$ to a vector variate Z following the standard multivariate normal distribution $N_k(0, I)$. With this, we can just generate N vector variates, $\{Z_j, j = 1, 2, \ldots, N\}$ only once from $N_k(0, I)$ and reuse them for all replications. Specifically, for a replication with sample mean $\hat{\mu}$ and sample covariance matrix $\hat{\Sigma}$, we transform the specification region by the transformation $T(\cdot) = \Sigma^{-1/2}(\cdot - \hat{\mu})$. When the specification region is a rectangle (or cube), we only need to transform the vertices and then reconstruct the specification region in the transformed space. Then we can compute $\hat{q}_i$s in (12) by

$$\hat{q}_i = \frac{\sharp\{Z_j \in A_i' \cap A'\}}{N} \quad \text{for} \quad i = 1, 2, \ldots, 2^k,$$

where A_i' is the ith hyperquadrant of R^k in the standard coordinate system, and A' is the transformed specification region $T(A)$.

For simplicity, we illustrate our method by examples in the bivariate case with rectangular specifications. The rectangular specification is the most widely used shape in real-life applications. Table II lists the distribution parameters and the specifications of four examples. For illustration, Figure 3 plots, for each case, a set of sample data with size $n = 100$, the rectangular specification region, and the two orthogonal lines crossed at the sample mean with the eigenvectors of $\hat{\Sigma}$ as their directions.

To evaluate how well $\hat{BC}_{\text{pk}}$ estimates BC_{pk}, we generate 1000 sets of data with size $n = 100$ for each case and compute $\hat{BC}_{\text{pk}}$ for each set of data with the aforementioned algorithm using $N = 1{,}000{,}000$. Tables III–VI present, respectively, for Cases 1–4, the true values of q_1, q_2, q_3, q_4, and BC_{pk} as well as the sample mean and sample standard deviation of 1000 values of $\hat{q}_1$, $\hat{q}_2$, $\hat{q}_3$, $\hat{q}_4$, and $\hat{BC}_{\text{pk}}$. The bias defined as the difference between the sample mean and the true value is also included. The results indicate that $\hat{BC}_{\text{pk}}$ is a reasonable estimator.

Table II. Parameters and specifications of four bivariate normal examples

	Distribution parameters					X_1 spec		X_2 spec	
	μ_1	σ_1^2	μ_2	σ_2^2	ρ	LSL_1	USL_1	LSL_2	USL_2
Case1	6.0	0.8	7.0	1.0	0.0	2.0	10.0	3.0	10.0
Case2	5.0	0.5	6.0	0.45	0.5	2.0	8.0	3.0	8.0
Case3	3.0	1.0	6.0	1.0	0.2	0.5	6.5	1.0	7.0
Case4	1.0	1.0	1.0	1.0	0.2	1.0	5.0	1.0	3.0

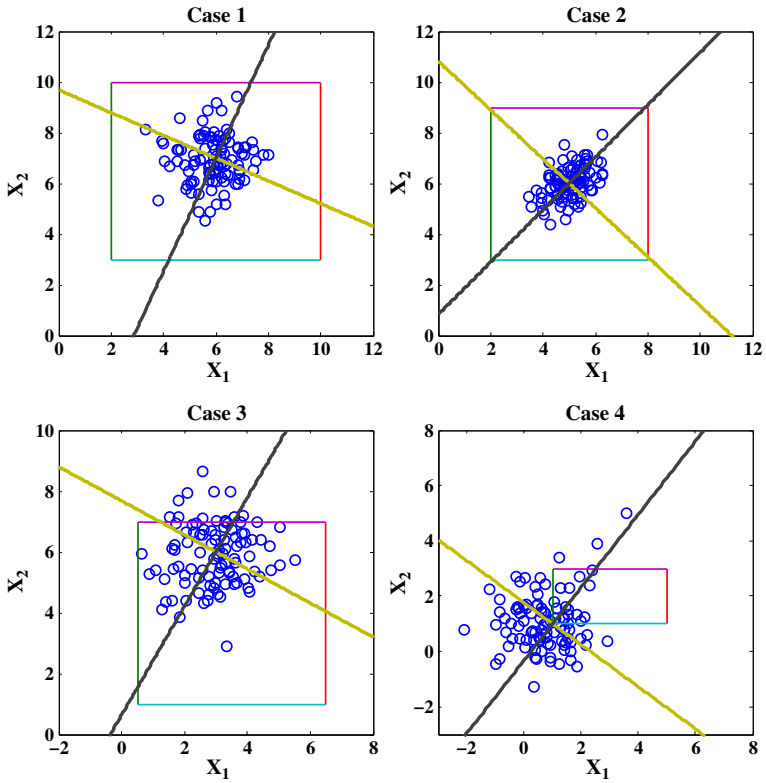

Figure 3. Illustration of the four cases in Table II, displaying 100 data points, the corresponding principal components, and the specification region

Table III. Estimation results of Case 1

	True value	Sample mean	Sample SD	Bias
q_1	0.2493360	0.2491962	0.0006310	0.0001398
q_2	0.2493280	0.2491763	0.0006431	0.0001517
q_3	0.2499820	0.2499745	0.0000264	0.0000075
q_4	0.2499860	0.2499727	0.0000302	0.0000133
BC_{pk}	1.0004445	0.9969328	0.07807013	0.0035117

Table IV. Estimation results of Case 2

	True value	Sample mean	Sample SD	Bias
q_1	0.2499920	0.2492297	0.0136783	0.0007623
q_2	0.2499970	0.2492439	0.0136790	0.0007531
q_3	0.2499870	0.2492214	0.0136778	0.0007656
q_4	0.2499990	0.2492467	0.0136792	0.0007523
BC_{pk}	1.3488170	1.3100525	0.1081182	0.0387645

Table V. Estimation results of Case 3

	True value	Sample mean	Sample SD	Bias
q_1	0.1613160	0.1606882	0.0177669	0.0006278
q_2	0.1784460	0.1778262	0.0143900	0.0006198
q_3	0.2462340	0.2459017	0.0023246	0.0003323
q_4	0.2499080	0.2498783	0.0001174	0.0000297
BC_{pk}	0.3084807	0.3094362	0.0459877	−0.0009555

Table VI. Estimation results of Case 4

	True value	Sample mean	Sample SD	Bias
q_1	0.2364030	0.2290143	0.0098276	0.0073887
q_2	0.0139380	0.0179137	0.0150866	−0.0039757
q_3	0.0000060	0.0198540	0.0008475	−0.0003036
q_4	0.0159930	0.0157176	0.0165061	−0.0038610
BC_{pk}	0.0000100	0.0005120	0.0014184	−0.0005020

2.6. *Statistical inference about MC_{pk}* via bootstrap approach

For statistical inference about any PCI, practitioners often emphasize the lower confidence bound of the PCI rather than the usual CI, viewing from the quality assurance aspect. Among PCIs, lower confidence bounds of indices in the C_{pk}-family are of particular interests for practitioners because the yield corresponding to the lower confidence bound represents the worst yield at a certain confidence level. So far as we know, no lower confidence bound has been developed for the C_{pk} index for processes of multiple characteristics in the literature.

Note that, with a set of process data, we can only obtain an $\hat{MC}_{pk}$. To infer anything about MC_{pk}, for example, its lower confidence bound, usually, we would need the distribution of $\hat{MC}_{pk}$ or have many $\hat{MC}_{pk}$s. Unfortunately, the distribution of $\hat{MC}_{pk}$ is analytically intractable, and repeating experiments to obtain a number of estimates is not possible or economical for most of the applications. Under such circumstances, the bootstrap approach introduced by Efron[24] is commonly used for statistical inferences. With the bootstrap method, one can repeat the resampling procedure many times to obtain 'bootstrap' estimates of the parameter of interest without specific model assumptions to infer about the population parameter.

We emphasize here that the purpose of the bootstrap is not to obtain a better parameter estimate because the bootstrap distribution is always centered around the statistic calculated from the data (here the value of $\hat{MC}_{pk}$), not the unknown population value (MC_{pk}). Rather, the bootstrap is useful and convenient for quantifying the behavior of a parameter estimate ($\hat{MC}_{pk}$), for example, obtaining its standard error/bias, or calculating CIs.

In this study, for making inferences on MC_{pk}, we also choose the bootstrap rather than other approaches to deal with this problem because it is simple, convenient to perform, and having sound statistical justifications for statistical inferences.

The bootstrap procedure can be briefly described as follows. Suppose that we have a random sample $\{X_1, X_2, \ldots, X_n\}$ of size n from a population with the c.d.f. F_θ, in which θ is the parameter of interest. Let $\hat{\theta}$ be an estimator of θ. Denote by $\{X_1^*, X_2^*, \ldots, X_n^*\}$ a resampled data set of size n obtained by resampling with replacement from $\{X_1, X_2, \ldots, X_n\}$. Then, X_j^*s are independent and identically distributed following the empirical distribution with the c.d.f. $F_n(x) = \frac{1}{n}\sum_{i=1}^{n} 1(X_i \leqslant x)$. Calculate $\hat{\theta}$ with this resampled data set and denote it by $\hat{\theta}^*$. Repeat this for B times, and obtain $\left\{\hat{\theta}_j^*, j = 1, 2, \ldots, B\right\}$. Then, we can have inferences about θ based on the bootstrap estimates $\hat{\theta}_1^*, \hat{\theta}_2^*, \ldots, \hat{\theta}_B^*$.

In this section, taking BC_{pk} as an illustrative example, we describe how to obtain lower confidence bounds for MC_{pk} via various bootstrap methods, including the *basic* bootstrap method, *percentile* bootstrap method, *standard* bootstrap method, and *bias-corrected percentile* bootstrap method. For more details about bootstrap methods, see, for example, Davison and Hinkly,[25] Efron,[24] Efron and Tibshirani,[26] and Carpenter and Bithell.[27]

1. *Basic bootstrap method*

Following Davison and Hinkly,[24] one can obtain an approximate $100(1-\alpha)\%$ CI of θ by the basic bootstrap method as

$$\left(2\hat{\theta} - \hat{\theta}^*_{([B(1-\frac{\alpha}{2})])},\ 2\hat{\theta} - \hat{\theta}^*_{([B(\frac{\alpha}{2})])}\right),$$

where $[x]$ stands for the nearest integer of x, $\hat{\theta}^*_{(i)}$ is the ith ordered estimate from the bootstrap procedure, and $\hat{\theta}$ is the estimate from the original sample. Analogously, an approximate $100(1-\alpha)\%$ lower confidence bound of the basic bootstrap method is $2\hat{\theta} - \hat{\theta}^*_{([B(1-\alpha)])}$.

2. *Standard bootstrap method*

The average and standard deviation of B bootstrap estimates $\hat{\theta}_1^*, \hat{\theta}_2^*, \ldots, \hat{\theta}_B^*$ are

$$\bar{\theta}^* = \frac{1}{B}\sum_{i=1}^{B}\hat{\theta}_i^* \quad \text{and} \quad S^* = \sqrt{\frac{1}{B-1}\sum_{i=1}^{n}\left(\hat{\theta}_i^* - \bar{\theta}^*\right)^2},$$

respectively. One can use normal approximation to obtain an approximate $100(1-\alpha)\%$ CI of θ based on the standard bootstrap method as

$$\left(\bar{\theta}^* - Z_{\frac{\alpha}{2}}S^*, \bar{\theta}^* + Z_{\frac{\alpha}{2}}S^*\right)$$

and the corresponding approximate $100(1-\alpha)\%$ lower confidence bound as $\bar{\theta}^* - Z_\alpha S^*$.

3. *Percentile bootstrap method*

The percentile bootstrap method simply takes the sample 100(α/2) and the 100(1 − α/2) percentage points as the confidence bounds to construct an approximate 100(1 − α)% CI as

$$\left(\hat{\theta}^*_{([B(\frac{\alpha}{2})])}, \hat{\theta}^*_{([B(1-\frac{\alpha}{2})])}\right)$$

and the corresponding approximate 100(1 − α)% lower confidence bound as $\hat{\theta}^*_{([B(\alpha)])}$.

4. *Bias-corrected percentile bootstrap method*

It is possible that the bootstrap distribution obtained using only a sample of the complete bootstrap distribution may be shifted higher or lower than would be expected; thus, the bias-corrected percentile (BCP) bootstrap method was suggested by Efron and Tibshirani[25] to correct this bias. First, using the distribution of $\hat{\theta}^*$, calculate the probability

$$p_0 = P\left(\hat{\theta}^* \leqslant \hat{\theta}\right)$$

by the proportion of $\hat{\theta}^*_i$s satisfying $\hat{\theta}^*_i \leqslant \hat{\theta}$. Second, calculate

$$\begin{aligned} z_0 &= \Phi^{-1}(p_0), \\ P_{L,\alpha/2} &= \Phi\left(2z_0 - z_{\alpha/2}\right), \\ P_{U,\alpha/2} &= \Phi\left(2z_0 + z_{\alpha/2}\right). \end{aligned}$$

Finally, an approximate 100(1 − α)% CI obtained by the BCP bootstrap method is

$$\left(\hat{\theta}^*_{([BP_{L,\alpha/2}])}, \hat{\theta}^*_{([BP_{U,\alpha/2}])}\right)$$

and the corresponding approximate 100(1 − α)% lower confidence bound is $\hat{\theta}^*_{([BP_{L,\alpha}])}$.

These four bootstrap methods have their own advantages and disadvantages, see Carpenter and Bithell.[26] Briefly speaking, the percentile method is simple to calculate and often works well, especially when the sampling distribution is symmetrical; however, it may not have the correct coverage when the sampling distribution is skewed. Both basic bootstrap and standard bootstrap CIs require statistics with small bias and sampling distributions close to normal. When bias or skewness is present in the bootstrap distribution, one can use BCP bootstrap method; the basic, standard, and percentile intervals are inaccurate under these circumstances unless the sample sizes are very large. Carpenter and Bithell[26] provided a practical guide on the use of bootstrap CIs, including guides on when they should be used, which method should be chosen, and how they should be implemented. Which bootstrap methods are proper for a particular application depends on the sampling distribution, sample size, bootstrap number, or even the original data.

For demonstration, we apply these four bootstrap methods to Case 1 example given in Table II, which has a BC_{pk} very close to 1.00. Consider various sample sizes $n = 30(10)100, 125(25)200, 250, 300$. For each generated sample, we use the algorithm described earlier to obtain a $\hat{BC}_{pk}$. Here, for the Monte Carlo integration, we generate $N = 1,000,000$ data from $N_2(0, I)$. We then perform the bootstrap resampling $B = 3000$ times to obtain 3000 bootstrap estimates of BC_{pk}. With these 3000 estimates, we obtain a lower confidence bound (LCB) for each of the four bootstrap methods. To see the performance of the proposed LCB, we repeat these steps for 300 times to obtain 300 LCBs.

To compare the four bootstrap methods, we consider three criteria: (i) the mean of LCB (the closer to the nominal value the better); (ii) the standard deviation of LCB (the smaller the better); and (iii) the coverage probability (the closer to the confidence level the better). Each of these three criteria has its own merit. As their sample version, Table VII lists the sample mean, sample standard deviation, and coverage rate of the simulated 300 LCBs obtained at 90% confidence level under various sample sizes n for each of the four bootstrap methods. To help us read the simulation results, for each sample size n, we highlight the mean LCB closest to 1.00, the smallest standard deviation, and the coverage rate closest to 90% among the four methods; we also 'teletype' the worst ones. From Table VII, we observe the following:

- It is clearly seen that the mean LCB becomes closer to the nominal value 1.00 and the standard deviation becomes smaller as data size n becomes larger for all bootstrap methods.
- The percentile method performs the best, and the basic method performs the worst under the criteria (i) and (ii); more specifically, the performance orderings of the four methods are percentile > standard > BCP > basic under both criteria.
- The coverage rates of the four methods are reasonable in general, but the ordering is mixed, no apparent patterns. The basic bootstrap method seems performing the worst (especially when n is large), whereas the other three methods seem not too much different.

We remark that the ordering based on empirical LCB values is not necessarily the actual ordering because of the estimation error. In summary, all four methods are reasonable methods with the percentile method being the best and the basic method being the worst. Therefore, we recommend the percentile bootstrap method for computing the LCB of MC_{pk}.

Table VII. The sample mean, sample standard deviation, and coverage rate of 300 lower confidence bounds at 90% confidence level for an example with $BC_{pk} \approx 1$

Data size	Sample mean	Sample SD	Coverage rate (%)	Sample mean	Sample SD	Coverage rate (%)
		Basic			Standard	
30	0.812937	0.16718	**86.33**	0.856004	0.13526	**86.33**
40	0.828009	0.13559	**89.33**	0.863823	0.11560	89.00
50	0.846850	0.12064	**87.00**	0.879382	0.10116	86.00
60	0.855107	0.10840	88.67	0.880893	0.09870	**89.33**
70	0.862006	0.09320	91.67	0.886200	0.08901	87.67
80	0.869648	0.08790	**90.33**	0.890566	0.08171	88.00
90	0.884494	0.08394	91.67	0.903152	0.07898	**90.33**
100	0.886191	0.07873	93.00	0.904637	0.07520	90.67
125	0.899050	0.06851	94.33	0.914252	0.06745	**89.67**
150	0.906501	0.06354	92.33	0.918361	0.06206	89.33
175	0.916951	0.05776	92.00	0.925228	0.05672	**90.33**
200	0.926768	0.05584	92.00	0.935849	0.05548	**90.33**
250	0.928409	0.04986	91.33	0.937738	0.04836	**90.00**
300	0.934398	0.04385	93.00	0.938921	0.04360	93.33
		Percentile			Bias-corrected percentile	
30	**0.862382**	**0.13089**	**86.33**	0.853172	0.14994	85.00
40	**0.869565**	**0.11272**	**89.33**	0.860984	0.12254	88.33
50	**0.883955**	**0.09887**	85.33	0.874425	0.10969	86.00
60	**0.885301**	**0.09680**	**89.33**	0.878285	0.10110	88.67
70	**0.890589**	**0.08901**	87.33	0.882519	0.09169	**89.00**
80	**0.894095**	**0.08039**	87.67	0.888119	0.08327	89.33
90	**0.906300**	**0.07792**	**90.33**	0.901452	0.08044	90.67
100	**0.907816**	**0.07405**	**90.33**	0.902246	0.07539	91.67
125	**0.916704**	**0.06675**	**89.67**	0.912058	0.06693	92.33
150	**0.920422**	**0.06145**	89.00	0.917068	0.06243	**89.67**
175	**0.926494**	**0.05673**	90.67	0.923867	0.05735	91.33
200	**0.937575**	**0.05518**	88.67	0.935379	0.05571	89.00
250	**0.938241**	**0.04828**	89.67	0.937381	0.04846	89.67
300	**0.940157**	**0.04361**	**92.00**	0.940005	0.04439	92.33

Bold emphasis indicates the (best) method with the lower confidence bound closest to 1.00, the least standard deviation, and the coverage rate closest to 90% under the three criteria, respectively; on the other hand, the teletyped numbers indicates the worst method among the four methods.

2.7. *Empirical distribution function of* $\hat{BC}_{pk}$

To acquire some idea about the sampling distribution of $\hat{BC}_{pk}$, we simulate 100,000 $\hat{BC}_{pk}$s for Case 1 ($BC_{pk} \approx 1.00$) and Case 2 ($BC_{pk} \approx 1.33$) examples in Table II by the algorithm described in Section 2.5 with sample data of size $n = 500$ and using $N = 10,000,000$ simulated $N_2(0, I)$ data for Monte Carlo integration.

Figure 4 displays the distributions of 100,000 $\hat{BC}_{pk}$s in the form of histograms for these two cases, which look fairly normal-like.

To see if $\hat{BC}_{pk}$ behaves similarly to a normal distribution, we further calculate the empirical cumulative distribution function of the simulated $\hat{BC}_{pk}$s and compare it with a normal distribution for each case. See Figure 5. In addition, Figure 6 presents the Q-Q plots of the 100,000 simulated $\hat{BC}_{pk}$s for both cases. These plots suggest that the sampling distribution of $\hat{BC}_{pk}$ is fairly close to a normal distribution.

3. Multivariate C_p index—a variation measuring process capability index

3.1. *Bivariate* C_p index: BC_p

In the univariate case, the index C_p is defined as

$$C_p = \frac{USL - LSL}{6\sigma},$$

which only accounts for the process variation and totally ignores the location of the process mean μ. So C_p is sometimes referred to as a variation measuring index. By their definitions, $C_{pk} \leqslant C_p$ and the equality holds only when $\mu = (LSL + USL)/2$, that is, when the process is well centered in the specification region, the most desirable location.

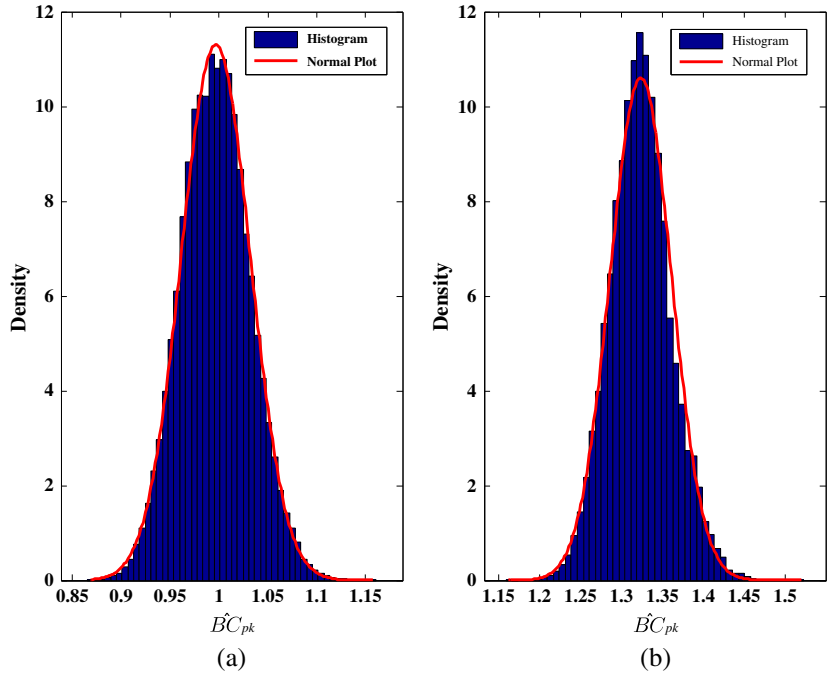

Figure 4. Histograms of 100,000 $\hat{BC}_{pk}$s with a normal curve for (a) $BC_{pk} \approx 1.00$ (b) $BC_{pk} \approx 1.33$

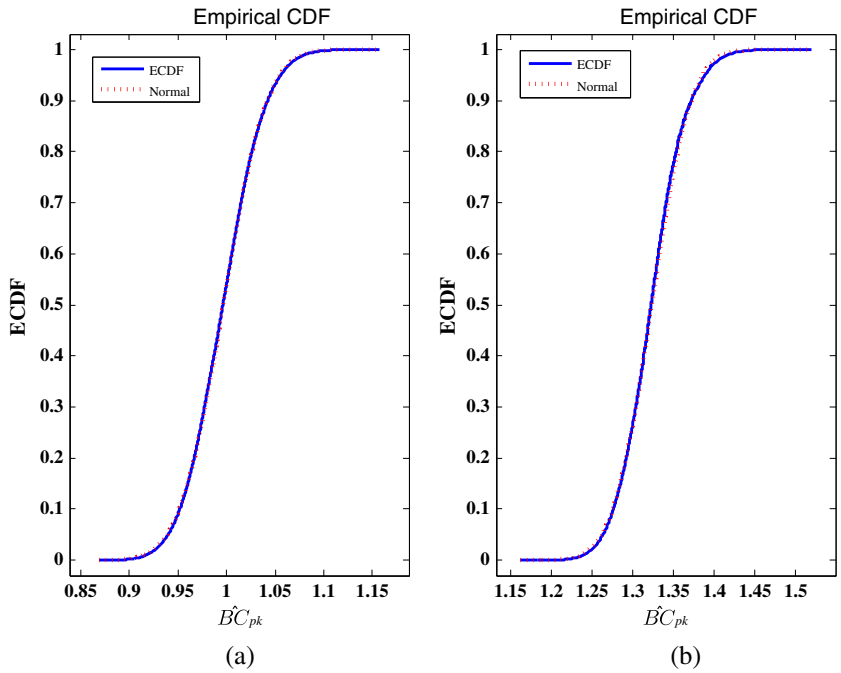

Figure 5. Comparing the empirical cumulative distribution function (c.d.f.) of 100,000 $\hat{BC}_{pk}$s with a normal distribution for (a) $BC_{pk} \approx 1.00$ and (b) $BC_{pk} \approx 1.33$

Because of this, Castagliola and Castellanos[22] defined a new bivariate C_p index, BC_p, as the maximum value of BC_{pk} over the process mean μ and the angle θ of the rotation matrix R that rotates the original axes to the two principal components (i.e., eigenvectors of Σ) as described earlier in Section 2.2. Specifically,

$$BC_p \equiv \max_{\mu,\theta} BC_{pk}. \tag{13}$$

Because BC_{pk} itself is defined as the minimum of the four values, $-\Phi^{-1}(2p_1)$, $-\Phi^{-1}(2p_2)$, $-\Phi^{-1}(2p_3)$, and $-\Phi^{-1}(2p_4)$, the maximum value of BC_{pk} is necessarily reached when $-\Phi^{-1}(2p_1) = -\Phi^{-1}(2p_2) = -\Phi^{-1}(2p_3) = -\Phi^{-1}(2p_4)$, that is, when $p_1 = p_2 = p_3 = p_4$ and $p \equiv p_1 + p_2 + p_3 + p_4$ is minimum; or equivalently when $q_1 = q_2 = q_3 = q_4$ and $q \equiv q_1 + q_2 + q_3 + q_4$ is maximum. As a result,

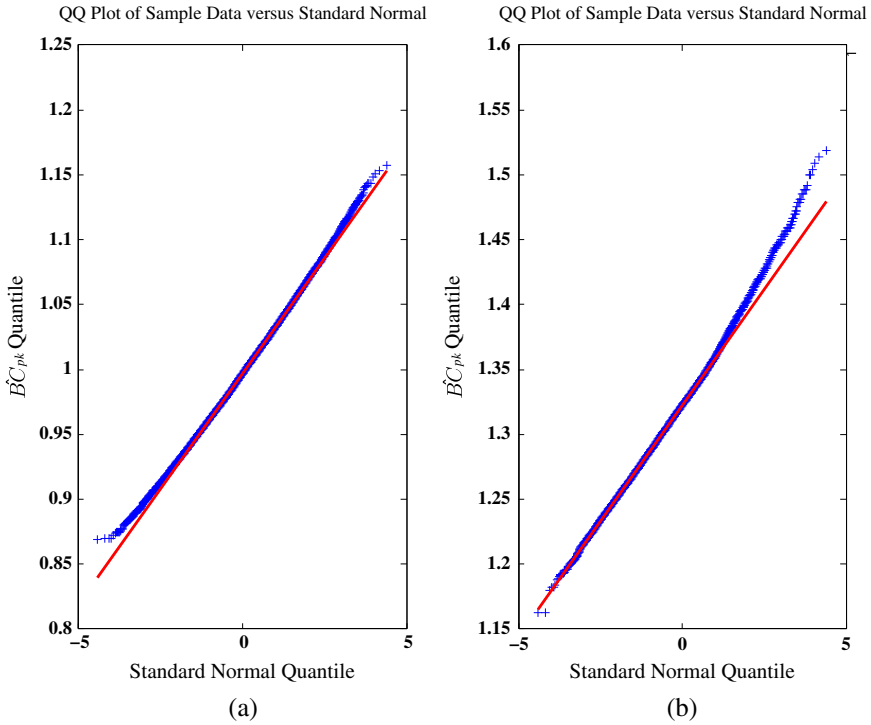

Figure 6. Q–Q plots of 100,000 $\hat{BC}_{pk}$s for (a) $BC_{pk} \approx 1.00$ and (b) $BC_{pk} \approx 1.33$

$$BC_p = -\frac{1}{3}\Phi^{-1}\left(2 \times \frac{p}{4}\right) = -\frac{1}{3}\Phi^{-1}\left(\frac{p}{2}\right) = -\frac{1}{3}\Phi^{-1}\left(\frac{1-q}{2}\right). \tag{14}$$

Then, it remains to find the μ and θ such that the corresponding process has the previously mentioned property. Castagliola and Castellanos[22] proposed a solution (in fact, a procedure) by letting $\mu_1 = (LSL_1 + USL_1)/2$, $\mu_2 = (LSL_2 + USL_2)/2$ and varying the rotation angle θ of the rotation matrix R to search for the optimal p. The definition and the procedure *seem* reasonable intuitively.

Unfortunately, the BC_p defined as in (13) is not scale-invariant, in the sense that the value of BC_p varies if we rescale the process variables X_1 and X_2, or simply use another unit for the variables. Let us take the four examples in Table II to demonstrate this scaling problem. We rescale each case by $X_1' = 2X_1$ and $X_2' = 3X_2$. Table VIII lists the parameters and specifications of each case after scaling. Table IX presents the values of BC_{pk} and BC_p along with the corresponding values of θ and p obtained by Castagliola and Castellanos's

Table VIII. Parameters and specifications of four examples after scaling

	Distribution parameters					X_1' spec		X_2' spec	
	μ_1	σ_1^2	μ_2	σ_2^2	ρ	LSL_1	USL_1	LSL_2	USL_2
Case1′	12.0	3.2	21.0	9.0	0.0	4.0	20.0	9.0	30.0
Case2′	10.0	2.0	18.0	4.05	0.5	4.0	16.0	9.0	27.0
Case3′	6.0	4.0	18.0	9.0	0.2	1.0	13.0	3.0	21.0
Case4′	2.0	4.0	3.0	9.0	0.2	2.0	10.0	3.0	9.0

Table IX. BC_p and BC_{pk} values of four examples before and after scaling

	BC_{pk}	BC_p		
Case 1	1.0004445	1.2528016	$\theta = 90°$,	$p = 0.0000428$
Case 1′	1.0004445	1.2098245	$\theta = 25°$,	$p = 0.0000710$
Case 2	1.3488170	1.3862485	$\theta = 0°$ (or 90°,180°, 270°),	$p = 0.0000080$
Case 2′	1.3488170	1.393727	$\theta = 170°$,	$p = 0.000007$
Case 3	0.3084807	0.9257124	$\theta = 0°$ (or 90°,180°, 270°),	$p = 0.0013710$
Case 3′	0.3084807	0.9334442	$\theta = 170°$,	$p = 0.0012763$
Case 4	0.0000100	0.3353143	$\theta = 45°$,	$p = 0.0786108$
Case 4′	0.0000100	0.3550567	$\theta = 75°$,	$p = 0.0716998$

procedure for all four cases. From Table IX, it is clearly seen that θ, p, and BC_p change their values after rescaling whereas BC_{pk} stays the same. The scale-invariance property of BC_{pk} is apparent because rescaling will not change the probability of the quality characteristic vector X being in each specification polygon Q_i.

In real practice, it is very common for people to use different units for quality characteristics. Any process assessment scheme definitely should not be affected by the unit used, which means, mathematically, a well-defined capability index should be invariant of scaling. Here, we propose a simple solution to fix this problem: rescale the data and the specifications such that the specification rectangle becomes a square centered at the origin (0,0), which in some sense is to 'equalize' the importance of the variables. Let the specification region be the rectangle $[LSL_1, USL_1] \times [LSL_2, USL_2]$. As an example, we can transform the quality characteristic vector $X=(X_1,X_2)^T$ into $X' = \left(X_1', X_2'\right)^T$ by $X_1' = \frac{1}{USL_1-LSL_1}\left(X_1 - \frac{USL_1+LSL_1}{2}\right)$ and $X_2' = \frac{1}{USL_2-LSL_2}\left(X_2 - \frac{USL_2+LSL_2}{2}\right)$. Then, the specification rectangle is transformed into the unit square $\left[-\frac{1}{2},\frac{1}{2}\right] \times \left[-\frac{1}{2},\frac{1}{2}\right]$. In fact, the requirement of the unit length is not necessary, a square centered at the origin is sufficient. Then BC_p becomes scale-invariant because the distribution of X' and the specification region will be the same no matter which scale was used originally.

Suppose X is a bivariate normal random vector following $N(\mu_1, \mu_2, \sigma_1^2, \sigma_2^2, \rho)$. Then, X' follows $N\left(\frac{1}{USL_1-LSL_1}\left(\mu_1 - \frac{USL_1+LSL_1}{2}\right), \frac{1}{USL_2-LSL_2}\left(\mu_2 - \frac{USL_2+LSL_2}{2}\right), \frac{\sigma_1^2}{(USL_1-LSL_1)^2}, \frac{\sigma_2^2}{(USL_2-LSL_2)^2}, \rho\right)$.

3.2. Estimation of BC_p

In this subsection, we first develop an algorithm to calculate $\hat{BC}_p$, and then derive an approximate normal distribution for $\hat{BC}_p$ by Taylor expansion. Based on this normal approximation, we will develop procedures for statistical inference about BC_p, including the following: (i) testing whether the process is capable or not by hypothesis testing; (ii) constructing a CI of BC_p to obtain the precision of the estimate; and (iii) providing a lower confidence bound for practical usage in quality assurance.

As mentioned earlier, in the univariate case, if we move the process mean μ to the middle of the two specification limits, then $C_p = C_{pk}$, that is, $C_p = max_\mu C_{pk}$. For the bivariate case, it is slightly more complicated because we need to center and scale the variables first and then find $max_\theta BC_{pk}$. By setting the transformed specification region to be $\left[-\frac{1}{2},\frac{1}{2}\right] \times \left[-\frac{1}{2},\frac{1}{2}\right]$, it is obvious that we should move the process mean to the origin. For computing efficiency, instead of rotating the process distribution for each θ to find/calculate BC_p by the Monte Carlo integration (i.e., *varying* the transformed process distribution against the *fixed* transformed specification region), we keep the distribution fixed and rotate the specification region so that only one set of N-simulated transformed process data is needed for all θ to perform Monte Carlo integration. Figure 7(a) shows the relative position of the square and the process distribution for $\theta = 0^\circ$ (or $90^\circ, 180^\circ, 270^\circ$) whereas Figure 7(b) shows that for $\theta = 45^\circ$ (or $135^\circ, 225^\circ, 315^\circ$).

Because BC_p is the maximum value of BC_{pk}, it is natural to repeatedly use the algorithm for calculating BC_{pk} to calculate $\hat{BC}_p$ as follows.

Algorithm for calculating $\hat{BC}_p$:

1. Transform process data by

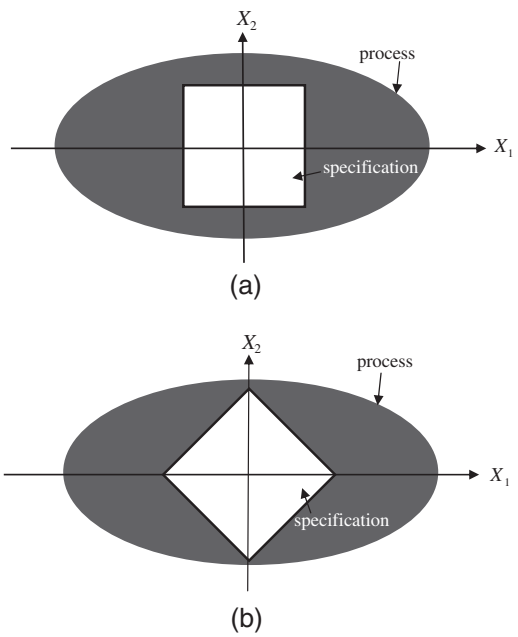

Figure 7. The two relative positions of the specification square w.r.t. the bivariate distribution when (a) $\theta = 0^\circ$ and (b) $\theta = 45^\circ$ (corresponding to BC_p)

$$X_1' = \frac{1}{USL_1 - LSL_1}\left(X_1 - \frac{USL_1 + LSL_1}{2}\right)$$

and

$$X_2' = \frac{1}{USL_2 - LSL_2}\left(X_2 - \frac{USL_2 + LSL_2}{2}\right)$$

so that the specification region becomes the unit square $\left[-\frac{1}{2},\frac{1}{2}\right] \times \left[-\frac{1}{2},\frac{1}{2}\right]$.

2. Compute the sample covariance matrix $\hat{\Sigma}$ from the transformed data.
3. Calculate the eigenvalues $\hat{\lambda}_1^2$ and $\hat{\lambda}_2^2$ of $\hat{\Sigma}$.
4. Loop θ over $0 \leqslant \theta < 360^\circ$ to find the optimal angle: for each candidate value of θ,

   - rotate the square $\left[-\frac{1}{2},\frac{1}{2}\right] \times \left[-\frac{1}{2},\frac{1}{2}\right]$ by an angle θ;
   - use the same approach for Monte Carlo integration as that in calculating $\hat{BC}_p$ to compute $\hat{q}_1(\theta)$, $\hat{q}_2(\theta)$, $\hat{q}_3(\theta)$, and $\hat{q}_4(\theta)$, the probabilities that a bivariate random vector following $N\left(0, 0, \hat{\lambda}_1^2, \hat{\lambda}_2^2, 0\right)$ falls in the rotated specification region intersecting the four quadrants, respectively;
   - then, compute $\hat{q}(\theta) = \hat{q}_1(\theta) + \hat{q}_2(\theta) + \hat{q}_3(\theta) + \hat{q}_4(\theta)$, the probability that the bivariate random vector falls in the rotated square (see Figure 7 for (a) $\theta = 0^\circ$ and (b) $\theta = 45^\circ$).

   Find an angle θ such that $\hat{q}(\theta)$ is maximized over $0 \leqslant \theta < 360^\circ$. Denote the optimal θ by θ^* and $\hat{q}(\theta^*)$ by $\hat{q}^*$.
5. Compute $\hat{BC}_p = -\frac{1}{3}\Phi^{-1}\left(\frac{1-\hat{q}^*}{2}\right)$.

In an earlier study, we applied this algorithm to various bivariate normal processes and found that we always got $\theta^* = 45^\circ$ for the optimal $\hat{q}^*$. Then, we started wondering: is it true that BC_p equals BC_{pk} when and only when the process mean is at the center of the specification square and the two axes of the process distribution are exactly the two crossed lines connecting the vertices of the square as depicted in Figure 7(b)? The answer is yes. To show this, first, it is fairly obvious to see that only two particular positions of the square can have $q_1 = q_2 = q_3 = q_4$ as depicted in Figure 7; that is, when θ is (i) 0° (also, $90^\circ, 180^\circ, 270^\circ$) as in Figure 7(a), or (ii) 45° (also, $135^\circ, 225^\circ, 315^\circ$) as in Figure 7(b). This observation was further confirmed by computer computation. Next, we show that $q(45^\circ) > q(0^\circ)$.

Because BC_{pk} is a function of the yield q, we first derive the formula for q. As before, by considering the relative position of the transformed process and specification region, we can assume, without loss of generality, that the process follows $N(0, 0, \lambda_1^2, \lambda_2^2, 0)$, and the specification square for $\theta = 0^\circ$ has vertices $\left(\sqrt{2}/2, 0\right)$, $\left(0, \sqrt{2}/2\right)$, $\left(-\sqrt{2}/2, 0\right)$, and $\left(0, -\sqrt{2}/2\right)$; see Figure 7(a). Denote the yields for the cases of $\theta = 0^\circ$ and $\theta = 45^\circ$ as a function λ_1 and λ_2 by $q_0(\lambda_1, \lambda_2)$ and $q_*(\lambda_1, \lambda_2)$, respectively. Then, given λ_1 and λ_2, for the case of $\theta = 0^\circ$, we have

$$q_0(\lambda_1, \lambda_2) = \left(2\Phi\left(\frac{1}{2\lambda_1}\right) - 1\right)\left(2\Phi\left(\frac{1}{2\lambda_2}\right) - 1\right),$$

because X_1 and X_2 are independent. For the case of $\theta = 45^\circ$, we have

$$\begin{aligned} q_*(\lambda_1, \lambda_2) &= 4\int_0^{\sqrt{2}/2}\int_0^{-x_1+\sqrt{2}/2} \frac{1}{2\pi\lambda_1\lambda_2} e^{-\frac{x_1^2}{2\lambda_1^2} - \frac{x_2^2}{2\lambda_2^2}} dx_2 dx_1 \\ &= 4\int_0^{\sqrt{2}/2} \frac{1}{\sqrt{2\pi}\lambda_1} e^{-\frac{x_1^2}{2\lambda_1^2}} \left(\Phi\left(\frac{-x_1 + \sqrt{2}/2}{\lambda_2}\right) - 1/2\right) dx_1 \\ &= 4\int_0^{\sqrt{2}/2} \phi\left(\frac{x_1}{\lambda_1}\right)\Phi\left(\frac{-x_1 + \sqrt{2}/2}{\lambda_2}\right) dx_1 - 2\Phi\left(\frac{\sqrt{2}}{2\lambda_1}\right) + 1. \end{aligned}$$

Because it is difficult to show that $q_0(\lambda_1, \lambda_2) < q_*(\lambda_1, \lambda_2)$ for all λ_1 and λ_2 analytically, we verify the claim by computation as follows. We calculate these two values by numerical integration for various values of λ_1 and λ_2. Figure 8 presents the ratio q_*/q_0 as a function of λ_1/λ_2 for $\lambda_1 = .25, .375, .5, 1, 2, 4, 8$ and $\lambda_1/\lambda_2 = 1, 2, \ldots, 100$. The solid line presents q_*/q_0 for $\lambda_1 = 1$, the three dashed lines are for $\lambda_1 = .25, .375, .5$, and the three dotted lines are for $\lambda_1 = 2, 4, 8$, respectively. It is clearly seen that the values of q_*/q_0 are all greater than 1.

Therefore, instead of looping over various values of θ to calculate the optimal $\hat{q}$, we can simply set $\theta^* = 45^\circ$ and calculate $\hat{BC}_p$ directly. This would save tremendous amount of computing time. Thus, we can simplify the computing algorithm by replacing the original Step 4 with the following Step 4*:

4*. Generate N bivariate normal variates from $N\left(0, 0, \hat{\lambda}_1^2, \hat{\lambda}_2^2, 0\right)$. Compute the proportion of the N bivariate data that fall in the unit square as depicted in Figure 7(b) to obtain $\hat{q}^*$.

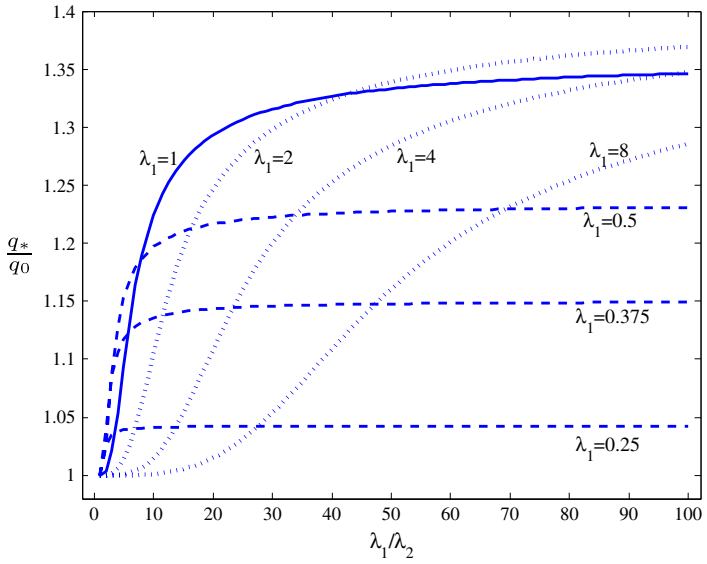

Figure 8. Ratio $q_*(\lambda_1, \lambda_2)/q_0(\lambda_1, \lambda_2)$ for λ_1 =.25,.375,.5, 1, 2, 4, 8 and $\lambda_1/\lambda_2 = 1, 2, \ldots, 100$

3.3. *Statistical inference about BC_p* via normal approximation

The exact distribution of $\hat{BC}_p$ is mathematically intractable. Fortunately, we can obtain a normal approximation to the distribution of $\hat{BC}_p$ by taking its first-order Taylor expansion as follows.

The partial derivatives of $q_*(\lambda_1, \lambda_2)$ with respective to λ_1 and λ_2 are, respectively,

$$\frac{\partial q_*(\lambda_1,\lambda_2)}{\partial \lambda_1} = 4\int_0^{\sqrt{2}/2} \phi\left(\frac{x_1}{\lambda_1}\right)\left(\frac{x_1^2}{\lambda_1^2}-\frac{1}{\lambda_1}\right)\Phi\left(\frac{-x_1+\sqrt{2}/2}{\lambda_2}\right)dx_1 + \phi\left(\frac{\sqrt{2}}{2\lambda_1}\right)\left(\frac{\sqrt{2}}{\lambda_1^2}\right),$$
$$\frac{\partial q_*(\lambda_1,\lambda_2)}{\partial \lambda_2} = 4\int_0^{\sqrt{2}/2} \phi\left(\frac{x_1}{\lambda_1}\right)\phi\left(\frac{-x_1+\sqrt{2}/2}{\lambda_2}\right)\left(\frac{x_1-\sqrt{2}/2}{\lambda_2^2}\right)dx_1,$$

which can be evaluated numerically when given λ_1 and λ_2.

Denote $Q_1(\lambda_1, \lambda_2) \equiv \frac{\partial q_*(\lambda_1,\lambda_2)}{\partial \lambda_1}$ and $Q_2(\lambda_1, \lambda_2) \equiv \frac{\partial q_*(\lambda_1,\lambda_2)}{\partial \lambda_2}$. Then, an approximate distribution of $\hat{BC}_p$ can be obtained as

$$N\left(BC_p, \frac{Q_1^2(\lambda_1,\lambda_2)\lambda_1^2 + Q_2^2(\lambda_1,\lambda_2)\lambda_2^2}{2\times 36n\left[\phi(3BC_p)\right]^2}\right) \tag{15}$$

by Taylor expansion. The derivation of (15) is given in the Appendix.

Plugging $\hat{\lambda}_i$ for λ_i, $i = 1, 2$, we can construct from the approximate normal distribution of $\hat{BC}_p$ an approximate 100(1-α)% CI as

$$\hat{BC}_p \pm Z_{\alpha/2}\frac{\left(Q_1^2\left(\hat{\lambda}_1,\hat{\lambda}_2\right)\hat{\lambda}_1^2 + Q_2^2\left(\hat{\lambda}_1,\hat{\lambda}_2\right)\hat{\lambda}_2^2\right)^{1/2}}{\sqrt{72n}\phi\left(3\hat{BC}_p\right)} \tag{16}$$

and an approximate 100(1$-\alpha$)% lower confidence bound as

$$\hat{BC}_p - Z_{\alpha}\frac{\left(Q_1^2\left(\hat{\lambda}_1,\hat{\lambda}_2\right)\hat{\lambda}_1^2 + Q_2^2\left(\hat{\lambda}_1,\hat{\lambda}_2\right)\hat{\lambda}_2^2\right)^{1/2}}{\sqrt{72n}\phi\left(3\hat{BC}_p\right)}, \tag{17}$$

where Z_α is the αth upper quantile of the standard normal distribution.

To investigate whether the process capability meets customers' demands or not, practitioners can perform hypothesis testing on BC_p. Consider the hypotheses

$$H_0 : BC_p \leqslant C \text{ (process is not capable)}$$
$$H_1 : BC_p > C \text{ (process is capable)}$$

where $C > 0$ is the preset acceptable capability level. A naive test can be conducted with the following test statistic:

$$Z^* = \frac{\sqrt{72n}\phi\left(3\hat{BC}_{\mathrm{p}}\right)\left(\hat{BC}_{\mathrm{p}} - C\right)}{\left(Q_1^2\left(\hat{\lambda}_1, \hat{\lambda}_2\right)\hat{\lambda}_1^2 + Q_2^2\left(\hat{\lambda}_1, \hat{\lambda}_2\right)\hat{\lambda}_2^2\right)^{1/2}}$$

and the decision making rule at the significance level α is

$$\begin{array}{c}\text{reject } H_0, \text{if } Z^* > Z_\alpha, \\ \text{do not reject } H_0, \text{if } Z^* \leqslant Z_\alpha.\end{array}$$

3.4. *The simulated examples*

We apply the proposed methods for BC_{p} to the four examples in Table II. To evaluate how well the estimation method performs, we generate 1000 sets of 100 bivariate normal data to obtain 1000 $\hat{BC}_{\mathrm{p}}$s for each case. Table X presents the sample mean and sample standard deviation of 1000 $\hat{BC}_{\mathrm{p}}$s as well as the true value of BC_{p} for each of Cases 1–4. With the sample size only 100, the estimation result is quite satisfactory. Table XI gives the 90% approximate LCB and 90% approximate CI of one simulated data set of size $n = 100$ for each case. The results indicate that the estimation method is satisfactory.

3.5. *Multivariate C_p* index: MC_p

The BC_{p} can be easily extended to the general case of k quality characteristics. After rescaling the data and the specifications as described earlier, the definition (13) becomes

$$MC_{\mathrm{p}} \equiv \max_{\mu, R} MC_{\mathrm{pk}},$$

where R is any rotation matrix in the Euclidean space R^k. Analogous to (14), MC_{p} satisfies

$$MC_{\mathrm{p}} = -\frac{1}{3}\Phi^{-1}\left(2^{k-1} \times \frac{p}{2^k}\right) = -\frac{1}{3}\Phi^{-1}\left(\frac{p}{2}\right) = -\frac{1}{3}\Phi^{-1}\left(\frac{1-q}{2}\right),$$

where q is the probability of a random normal vector with mean 0 and covariance matrix $\Sigma = \mathrm{diag}(\lambda_1, \lambda_2, \ldots, \lambda_k)$ falling in the origin-centered unit cube with the 2^k vertices all at axes, analogous to Figure 7(b).

4. Three real-life application examples

For demonstration, we employ our estimating methods given in the last two sections to three real-life industrial examples. The first two examples were described in Chen[12] involving bivariate processes, and the third one involves a trivariate process described in Pan *et al*.[28]

The first example was originally presented by Sultan[29] regarding an industrial process in which the Brinell hardness (X_1) and the tensile strength (X_2) are the quality characteristics. The Chen–Sultan's data consist of 25 samples taken from a process with the specifications for hardness and tensile strength being [112.7, 241.3] and [32.7, 73.3], respectively. Figure 9 depicts the data and the

Table X. Summary of 1000 $\hat{BC}_{\mathrm{p}}$s

Case	True value	Sample mean	Sample SD	Bias
1	1.245320	1.2453743	0.0692768	−0.000054
2	1.404933	1.404937	0.0882426	−0.000004
3	0.927604	0.9277373	0.0532411	−0.000133
4	0.326505	0.3280435	0.0230090	−0.001539

Table XI. 90% approximate lower confidence bound and confidence interval of BC_{p} from one data set

Case	LCB	CI
1	1.183757	[1.166305, 1.324336]
2	1.350439	[1.334990, 1.474876]
3	0.870863	[0.854778, 1.000430]
4	0.298699	[0.290817, 0.362191]

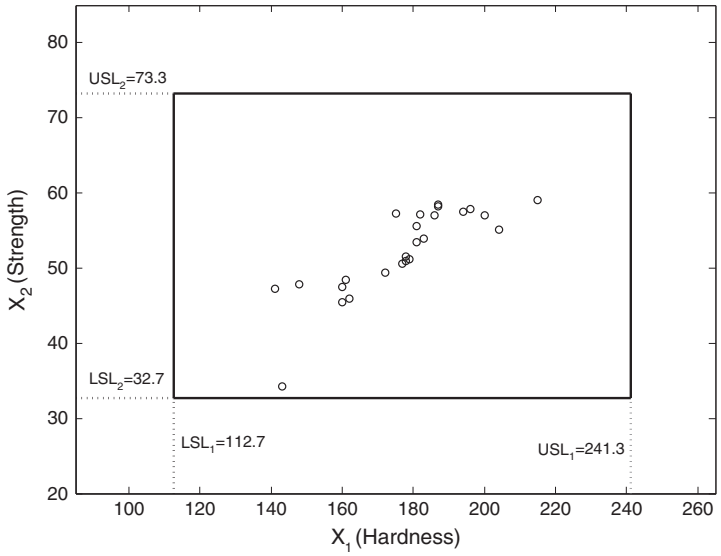

Figure 9. Data and specification region of Chen–Sultan's example

specification region. Table XII presents the estimate $\hat{BC}_{pk}$ along with the corresponding 90% CIs and 90% lower confidence bounds obtained by employing the four bootstrap methods with $B = 3000$ for the first example. Based on the $\hat{BC}_{pk}$ value of 1.050281, we can obtain by inequality (7) the estimated upper bound of the nonconforming rate to be 1628 ppm. Also, taking the LCB of the percentile bootstrap method as an example, with LCB = 0.7977719, by inequality (8), we can say that, with 90% confidence, the product yield is at least 98.3303%.

The second example was originally presented by Pal[13] regarding a manufacturing process of a bobbin with the height (X_1) and the weight (X_2) as quality characteristics. In this example, one hundred samples were taken from a process with the specification [40, 42] for height and [44, 46.5] for weight. The data and the specification region are displayed in Figure 10. The results of this example are presented in Table XIII. For this example, the $\hat{BC}_{pk} = 0.9610820$, which leads to an estimated upper bound of the nonconforming rate of 3936 ppm. Also, with the LCB of the percentile bootstrap method being 0.8825650, one can conclude that the yield of the product is at least 99.1896% with 90% confidence.

As to BC_p, by our efficient algorithm given in Subsection 3.2 (with Step 4*), for Chen–Sultan's example, we obtain $\hat{BC}_p = 1.1228071$ with the optimal $\hat{p} = 0.0001890$. Based on the normal approximation, (16) gives a 90% CI (0.8577761, 1.3878381) and (17) gives a 90% lower confidence bound (0.9163140). Similarly, for Pal's data, we obtain $\hat{BC}_p = 1.1890221$ with the optimal $\hat{p} = 0.0000903$, an approximate 90% CI (1.0748297, 1.3032146) and an approximate 90% lower confidence bound (1.1000516).

The third example is related to the example presented in Pan and Lee[11] regarding the solder paste stencil printing process, a cost-effective process that has been widely used in traditional high-volume surface mount assembly. For more descriptions about the process, see Pan *et al.*[28] In this process, solder-deposited volume (X_1), area (X_2), and height (X_3) are the three quality characteristics with high correlation. There are two kinds of stencils (of the same pattern) with thickness, 0.1 mm (4mil) and 0.15 mm (6mil) (1mil = 0.0254 mm). And there are five different aperture sizes, 30, 25, 20, 16, and 12 (mil). Pan and Lee[11] considered a $QFP_{4mil,\,30}$ process to demonstrate the effectiveness of their new multivariate PCIs, where $QFP_{4mil,\,30}$ represents that the process is for quad flat package (QFP), one of the advanced packages, with the stencil thickness as 4mil and aperture size as 30. The specifications and target values for this $QFP_{4mil,\,30}$ process are given in Table XIV. The authors kindly provided us with 150 measurements (not the same set of data as in Pan and Lee[11]) from the same process. Figure 11 displays the 150 data points and the specification region. We first check if the process follows a multivariate normal distribution by applying the Shapiro–Wilk normality test to these measurements, which

Table XII. BC_{pk} estimate, 90% confidence intervals, and 90% bootstrap lower confidence bounds of Chen–Sultan's example

$\hat{BC}_{pk} = 1.050281$			
$\hat{p}_1$	$\hat{p}_2$	$\hat{p}_3$	$\hat{p}_4$
0.000312	0.000043	0.000407	0.00005
90% confidence interval			
Basic	Standard	Percentile	Bias-corrected percentile
(0.7543558, 1.3818883)	(0.7196855, 1.3147242)	(0.7186737,1.3462062)	(0.8036442,1.4171286)
90% bootstrap lower confidence bound			
Basic	Standard	Percentile	Bias-corrected percentile
0.8451777	0.7853992	0.7977719	0.8544017

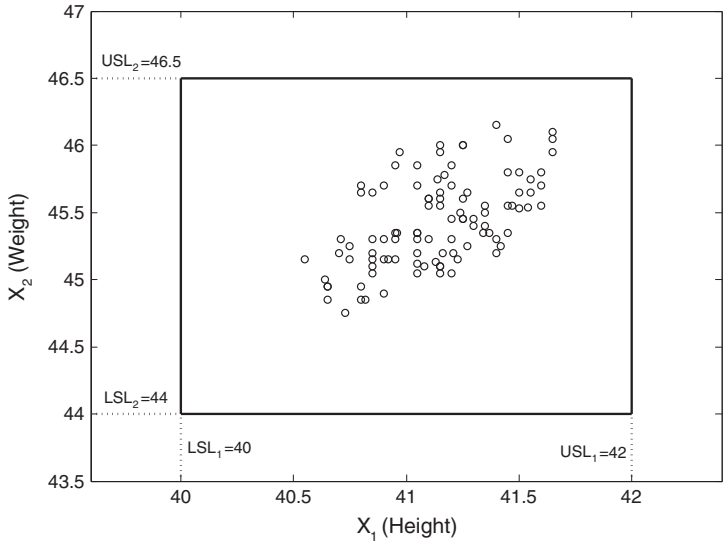

Figure 10. Data and specification region of Pal's example

Table XIII. BC_{pk} estimate, 90% confidence intervals, and 90% bootstrap lower confidence bounds of Pal's example

$\hat{BC}_{pk} = 0.9610820$			
$\hat{p}_1$	$\hat{p}_2$	$\hat{p}_3$	$\hat{p}_4$
0.000984	0.000083	0.000011	0.000081
90% confidence interval			
Basic	Standard	Percentile	Bias-corrected percentile
(0.8523437,1.0597296)	(0.8581923,1.0663559)	(0.8624344,1.0698203)	(0.8641023,1.0719583)
90% bootstrap lower confidence bound			
Basic	Standard	Percentile	Bias-corrected percentile
0.8778255	0.8811811	0.8825650	0.8842324

Table XIV. The target values and specifications for $QFP_{4mil,30}$ process

Quality characteristic	Target	*USL*	*LSL*
Deposited volume (X_1)	0.0787	0.10250	0.0549
Deposited area (X_2)	0.7870	0.96870	0.6052
Deposited height (X_3)	0.1000	0.12765	0.07235

gives a *p*-value of 0.8489; so that the normality holds. The sample mean vector and the sample covariance matrix are, respectively, $\bar{X}^T = (0.075859,\ 0.817971,\ 0.097080)$ and

$$S = \begin{pmatrix} 0.0000250 & 0.0002601 & 0.0000012 \\ 0.0002601 & 0.0028808 & -0.0000079 \\ 0.0000012 & -0.0000079 & 0.0000151 \end{pmatrix}.$$

Applying the proposed procedures to this dataset, we obtain the estimation results (presented in Table XV) for MC_{pk}, including the estimate $\hat{MC}_{pk}$ and the 90% CI/LCB obtained via bootstrap with $B = 3000$. With $\hat{MC}_{pk} = 0.9355062$, the estimated upper bounds of the nonconforming rates is 5008 ppm by inequality (10). Again, taking the LCB of the percentile bootstrap method as an example, with LCB = 0.8620695, by the first inequality in (11), we can say that, with 90% confidence, the yield of the product is at least 99.4992%. As to MC_p, by extending our efficient algorithm given in Subsection 3.2 to three dimensions (see Subsection 3.5 for the extension of Step 4*), we obtain $\hat{MC}_p = 1.1615466$ with the optimal $\hat{p} = 0.0000616$.

For practitioners' convenience, MATLAB (MathWorks, Natick, MA, USA) programs for computing the CIs and lower confidence bounds using the bootstrap approach are provided in http://www.stat.nctu.edu.tw/~jjhs/MPCI.zip or upon request.

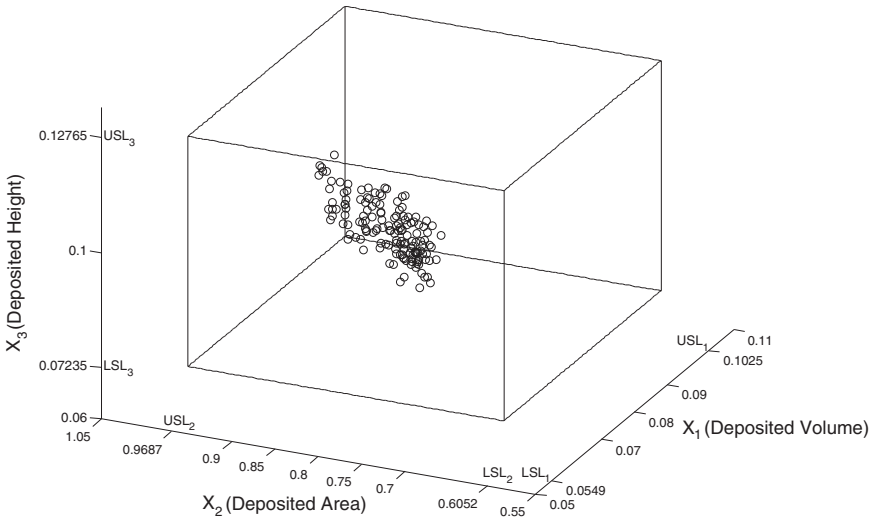

Figure 11. Data and specification region of stencil printing example

Table XV. MC_{pk} estimate, 90% confidence intervals, and 90% bootstrap lower confidence bounds of stencil printing example

$\hat{MC}_{pk} = 0.9355062$

$\hat{p}_1$	$\hat{p}_2$	$\hat{p}_3$	$\hat{p}_4$	$\hat{p}_5$	$\hat{p}_6$	$\hat{p}_7$	$\hat{p}_8$
0.000005	0.000011	0.000015	0.000014	0.000597	0.000602	0.000611	0.000626

90% confidence interval

Basic	Standard	Percentile	Bias-Corrected Percentile
(0.8241617,1.0277553)	(0.8362759,1.0406581)	(0.8432572,1.0468508)	(0.8447718,1.0490951)

90% bootstrap lower confidence bound

Basic	Standard	Percentile	Bias-corrected percentile
0.8513668	0.8588471	0.8620695	0.8636374

5. Conclusion

In this paper, we studied the bivariate PCIs, BC_{pk} and BC_p, proposed by Castagliola and Castellanos[22] and extended their notion to processes of more than two quality characteristics.

We established a link between BC_{pk} and the process yield by showing that the same inequality as in the univariate case holds, that is, $2\Phi(3BC_{pk}) - 1 \leqslant$ %yield. This lower bound provides a measure for quality assurance. With the same notion of BC_{pk}, we defined an index MC_{pk} for processes of more than two characteristics and proved that the lower bound inequality $2\Phi(3MC_{pk}) - 1 \leqslant$ %yield also holds. We also provided a new algorithm for computing the natural estimate $\hat{MC}_{pk}$ of MC_{pk}, which is more efficient than the algorithm provided for the bivariate case by Castagliola and Castellanos.[22] Moreover, the new algorithm can be used for processes with more general specification regions. For statistical inference, we utilized the bootstrap approach to obtain a lower confidence bound of BC_{pk}. Among the four popular bootstrap methods under study, we recommend the percentile bootstrap method.

For BC_p, we found that the original definition given in Castagliola and Castellanos[22] is not scale-invariant. We proposed a simple preprocessing step to fix the problem. By finding the exact situation when $BC_{pk} = BC_p$ (also for $MC_{pk} = MC_p$), we developed an efficient algorithm for computing the natural estimate of BC_p, which is a lot faster than the method given in Castagliola and Castellanos.[22] We further derived an approximate normal distribution for $\hat{BC}_p$ by taking its first-order Taylor expansion. This enabled us to derive statistical procedures for making inferences about process capability based on data, including hypothesis testing, confidence interval, and lower confidence bound.

Our simulation studies indicated that the sampling distribution of $\hat{BC}_p$ is fairly close to a normal distribution. If one could find a suitable normal approximation for it, then statistical inferences about BC_{pk} based on the normal approximation would be more computationally efficient and perhaps more statistically efficient than that obtained by the bootstrap approach.

Acknowledgements

The authors would like to express their gratitude to the editor and an anonymous referee for the careful review and constructive suggestions. The work was supported in part by the National Research Council of Taiwan, Grant No. NSC97-2118-M-009-002-MY2 and NSC99-2118-M-009-003-MY2.

References

1. Kane VE. Process capability indices. *Journal of Quality Technology* 1986; **18**(1):41–45.
2. Chan LK, Cheng SW, Spring FA. A new measure of process capability: C_{pm}. *Journal of Quality Technology* 1988; **20**(3):162–175.
3. Pearn WL, Kotz S, Johnson NL. Distributional and inferential properties of process capability indices. *Journal of Quality Technology* 1992; **24**(4):216–231.
4. Kotz S, Johnson NL. *Process Capability Indices*. Chapman and Hall: London, 1993.
5. Kotz S, Lovelace CR. *Process Capability Indices in Theory and Practice*. Arnold: London, 1998.
6. Pearn WL, Kotz S. *Encyclopedia and Handbook of Process Capability Indices: A Comprehensive Exposition of Quality Control Measures*. World Scientific, Hackensack: New Jersey, 2006.
7. Chan LK, Cheng SW, Spring FA. Multivariate measure of process capability. *Journal of Modeling and Simulation* 1991; **11**(1):1–6.
8. Hubele HF, Shahriari H, Cheng CS. A bivariate process capability vector. In *Statistical Process Control in Manufacturing*, Keats JB, Montgomery DC (eds). Marcel Dekker: New York, 1991; 299–310.
9. Shahriari H, Hubele NF, Lawrence FP. A multivariate process capability vector. *Proceedings of the 4th Industrial Engineering Research Conference, Institute of Industrial Engineers* 1995; 304–309.
10. Taam W, Subbaiah P, Liddy JW. A note on multivariate capability indices. *Journal of Applied Statistics* 1993; **20**(3):339–351.
11. Pan JN, Lee CY. New capability indices for evaluating the performance of multivariate manufacturing processes. *Quality and Reliability Engineering International* 2010; **26**(1):3–15.
12. Chen H. A multivariate process capability index over a rectangular solid tolerance zone. *Statistica Sinica* 1994; **4**(2):740–758.
13. Pal S. Performance evaluation of a bivariate normal process. *Quality Engineering* 1999; **11**(3):379–386.
14. Bothe DR. Composite capability index for multiple product characteristics. *Quality Engineering* 1999; **12**(2):253–258.
15. Wang FK, Hubele NF, Lawrence FP, Miskulin JD, Shahriari H. Comparison of three multivariate process capability indices. *Journal of Quality Technology* 2000; **32**(3):263–275.
16. Wang FK, Chen JC. Capability index using principal component analysis. *Quality Engineering* 1998–1999; **11**(1):21–27.
17. Wang FK, Du T. Using principal component analysis in process performance for multivariate data. *Omega: The International Journal of Management Science* 2000; **28**(2):185–194.
18. Shinde RL, Khadse KG. Multivariate process capability using principal componet analysis. *Quality and Reliability Engineering International* 2009; **25**(1):69–77.
19. Shinde RL, Khadse KG. A review and comparison of some multivariate process capability indices based on fraction conforming interpretation. *Statistical Methods* 2005; **7**:95–115.
20. Gonzalez I, Sanchez I. Capability indices and nonconforming proportion in univariate and multivariate processes. *International Journal of Advanced Manufacturing Technology* 2009; **44**(9):1036–1050.
21. Boyles RA. The Taguchi capability index. *Journal of Quality Technology* 1991; **23**(1):17–26.
22. Castagliola P, Castellanos JG. Capability indices dedicated to the two quality characteristics case. *Quality Technology & Quantitative Management* 2005; **2**(2):201–220.
23. Golub GH, Van Loan CF. *Matrix Computations* (2nd edn). The Johns Hopkins University Press, Baltimore: Maryland, 1989.
24. Efron B. Bootstrap methods: another look at the jackknife. *The Annals of Statistics* 1979; **7**(1):1–26.
25. Davison AC, Hinkly DV. *Bootstrap Methods and their Application*. Cambridge University Press: United States of America, 1997.
26. Efron B, Tibshirani RJ. Bootstrap methods for standard errors, confidence interval, and other measures of statistical accuracy. *Statistical Science* 1986; **1**(1):54–77.
27. Carpenter J, Bithell J. Bootstrap confidence intervals: when, which, what? A practical guide for medical statisticians. *Statistics in Medicine* 2000; **19**(9):1141–1164.
28. Pan J, Tonkay GL, Storer RH, Sallade RM, Leandri DJ. Critical variables of solder paste stencil printing for Micro-BGA and fine-pitch QFP. *IEEE Transactions on Electronics Packaging Manufacturing* 2004; **27**:125–132.
29. Sultan TI. An acceptance chart for raw materials of two correlated properties. *Quality Assurance* 1986; **12**(3):70–72.
30. Anderson TW. *An Introduction to Multivariate Statistical Analysis* (3rd edn). Wiley and Sons, Hoboken: New Jersey, 2003.

Appendix A

Derivation of the normal approximation given in (15)

Let $f(q) = BC_p = -\frac{1}{3}\Phi^{-1}\left(\frac{1-q}{2}\right)$. Denote $\hat{q} \equiv q\left(\hat{\lambda}_1, \hat{\lambda}_2\right)$. Then, $f(\hat{q}) = \hat{BC}_p$. Expanding $f(\hat{q})$ at q by Taylor expansion, we have

$$\begin{aligned} \hat{BC}_p &\approx -\frac{1}{3}\Phi^{-1}\left(\frac{1-q}{2}\right) + \frac{1}{6\phi\left(\Phi^{-1}\left(\frac{1-q}{2}\right)\right)}(\hat{q}-q) \\ &= BC_p + \frac{1}{6\phi\left(3BC_p\right)}(\hat{q}-q). \end{aligned} \tag{A.1}$$

Because $\hat{\lambda}_i$s are eigenvalues of the sample covariance matrix $\hat{\Sigma}$, by Anderson[30] (pages 473–474), we have

$$\sqrt{n}\left(\begin{bmatrix}\hat{\lambda}_1 \\ \hat{\lambda}_2\end{bmatrix} - \begin{bmatrix}\lambda_1 \\ \lambda_2\end{bmatrix}\right) \xrightarrow{d} N\left(0, \begin{bmatrix}\frac{1}{2}\lambda_1^2 & 0 \\ 0 & \frac{1}{2}\lambda_2^2\end{bmatrix}\right)$$

as $n \to \infty$ Then, by Theorem 4.2.3 of Anderson,[30]

$$\sqrt{n}\left(q\left(\hat{\lambda}_1, \hat{\lambda}_2\right) - q(\lambda_1, \lambda_2)\right) \xrightarrow{d} N\left(0, \frac{1}{2}\left(Q_1^2(\lambda_1, \lambda_2)\lambda_1^2 + Q_2^2(\lambda_1, \lambda_2)\lambda_2^2\right)\right)$$

as $n \to \infty$. Now denoting $Z_q \equiv \sqrt{n}\left(q\left(\hat{\lambda}_1, \hat{\lambda}_2\right) - q(\lambda_1, \lambda_2)\right)$, we have, by (A.1),

$$\hat{BC}_p \approx BC_p + \frac{1}{6\sqrt{n}\phi(3BC_p)} Z_q$$

and (15) is derived.

Authors' biographies

Jyh-Jen Horng Shiau is currently a full professor in the Institute of Statistics at National Chiao Tung University, Taiwan. She holds a BS in Mathematics from National Taiwan University, Taipei, Taiwan, an MS in Applied Mathematics from the University of Maryland Baltimore County, an MS in Computer Science and PhD in Statistics from the University of Wisconsin-Madison. Formerly, she taught at Southern Methodist University, the University of Missouri at Columbia, and National Tsing Hua University, and worked at AT&T Bell Laboratories before she moved to Taiwan. She is a former managing editor of an international journal *Quality Technology & Quantitative Management* (2004-2006). Her primary research interests include industrial statistics, nonparametric and semiparametric regression, and functional data analysis. She is a lifetime member of the International Chinese Statistical Association.

Chia-Ling Yen received her PhD degree in Statistics from National Chao-Tung University in 2008. Her research interests include multivariate analysis and statistical process control.

W. L. Pearn received the PhD degree in Operations Research from the University of Maryland, College Park. He is a professor of Operations Research and Quality Assurance at National Chiao-Tung University (NCTU), Hsinchu, Taiwan, China. He was with AT&T Bell Laboratories as a member of the quality research staff before joining NCTU. His research interests include process capability, network optimization, and production management.

Wan-Tse Lee received her master's degree in Statistics from National Chao-Tung University in 2009. She is currently working as a quality engineer in AU Optronics Corporation (AUO) in the Hsinchu Science and Industrial Park, Hsinchu, Taiwan. Her research interests include process capability and statistical process control.